Advances in Industrial and Manufacturing Engineering 5 (2022) 100091

Contents lists available at ScienceDirect

Advances in Industrial and Manufacturing Engineering

journal homepage: www.sciencedirect.com/journal/advances-in-industrial-and-manufacturing-engineering

Transition between flow-drill screwing systems considering joining process and joint characteristics

Stephan Altvater *, Sebastian P. Sikora **, Tjark Siefkes

German Aerospace Centre (DLR), Institute of Vehicle Concepts, Pfaffenwaldring 38-40, 70569, Stuttgart, Germany

ARTICLE INFO

Keywords:
Flow-drill screwing
Joint characterization
Multi-material design
Mechanical testing

ABSTRACT

Flow-drill screwing is one of the key joining technologies for car body structures in multi-material lightweight design. In the course of technological developments and subsequent volume production of a product, different assets are used to obtain the same joints, assuming that similar processes yield the same joint characteristics. Since a simple transfer of the process parameters for joining the same materials is usually not possible, a remarkable experimental effort is required to meet manufacturing requirements. In this study the transition to an enhanced flow-drill screwing system and its effects on the joint is investigated. For this purpose, two flow-drill screwing systems typically used in the automotive industry are considered. An application-oriented approach for determining the joining parameters is shown. First, the optimal joining parameters for the target system were determined based on the process curves and parameters of the initial system by fulfilling the requirements for the joint. The joints were evaluated by using cross sections and single-lap shear tests. On this basis, the results of both flow-drill screwing systems were compared. Due to the further development of the flow-drill screwing system the process times can be significantly shortened while achieving the same mechanical properties and better process control at the same time.

1. Introduction

The (European) environmental legislation for greenhouse gas emissions as well as increasing costs for raw materials and energy are today's main challenges, the diverse industrial branches have to deal with. The implementation of competitive and energy-efficient process routes is essential to be successful on the global markets, especially for strongly affected industries like the automotive sector. To fulfill the ambitious legal requirements for CO_2 emissions, beyond the development of improved or new powertrain concepts, a significant reduction of the vehicle weight is necessary (Friedrich, 2013; Schindler and Sievers, 2008). Weight reduction in the car body structures often focuses on the implementation of various lightweight materials in order to exploit their specific benefits within the design in a targeted manner. Mixed metallic components (e.g. steel-aluminum) as well as hybrid structures (e.g. metal-composites) are developed, which significantly contribute to resource efficiency by weight reduction, while improving the stiffness and crash performance of the car body at reasonable costs (Friedrich, 2013; Schindler and Sievers, 2008). In addition, profile intensive design methods increasingly require accessibility to the joint from one side. Due to the dissimilar properties of the materials, suitable and cost-efficient joining technologies and systems are necessary (Groche et al., 2014; Martinsen et al., 2015).

Different assets are used to obtain the same joints, e.g. at different production sites, assuming that similar processes yield the same joint characteristics. Moreover, the joining systems are regularly further developed to improve the joining results, meet customer requirements as well as introduce technological enhancements. The switch to an enhanced joining system, which is called *target* system (TS) in this paper, requires the modification of the joining parameters, applied with the *initial* system (IS). Theoretically, this calibration is necessary for every specific material combination. Since a simple transfer of the process parameters for joining the same materials is usually not possible, due to various influencing variables (actuators, sensors, adjustable process parameters), a remarkable experimental effort is required to meet manufacturing requirements.

In this work, on the basis of two different flow-drill screwing systems, a methodical procedure for the transition to a further developed flow-

Abbreviations: Target system, TS; Initial system, IS; Single-lap shear, SLS.

* Corresponding author.
** Corresponding author.
E-mail addresses: stephan.altvater@dlr.de (S. Altvater), sebastian.sikora@dlr.de (S.P. Sikora).

https://doi.org/10.1016/j.aime.2022.100091
Received 20 April 2022; Received in revised form 15 June 2022; Accepted 2 July 2022
Available online 14 July 2022

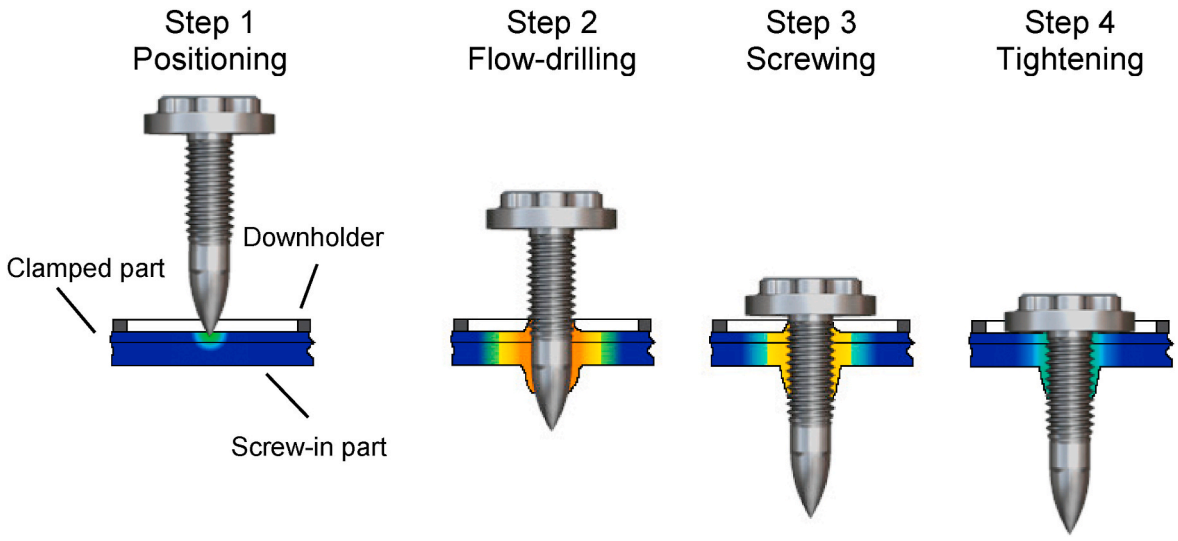

Fig. 1. Schematic representation of the steps during the flow-drill screwing process. Displayed at the end of each step and similar to the adjustable process steps of the target system.

drill screwing system is shown exemplarily. Challenges and differences of resulting joints with respect to processes as well as characteristics are discussed.

1.1. State of the art

Flow-drill screwing is a common joining technology used in the premium automotive industry. By this mechanical joining technique panel sheets, extrusions, castings or combinations of these can be joined by a screw, that extrudes the material and forms a thread. Furthermore, the use of profile-intensive design methods also increases the proportion of joints with one-sided accessibility. One big advantage of the flow-drill screwing technology is that tool access is only required from one side of the part. This characteristic enables the joining method to be used in configurations where other joining technologies cannot be applied. In addition, the connection can be released again non-destructively. This is particularly advantageous in the case of repair and recycling.

In literature, the joining process is typically divided into six steps (Hahn and Freymüller, 2017; Sønstabø et al., 2015; Küting and Hahn, 2004). For better understanding and consistency in this paper, the process steps shown in Fig. 1 are displayed according to the adjustable process steps of the target system. In the first step the joining element is positioned at the spot to be joined, accelerated to a high rotation speed and loaded with an axial force in the joining direction (Step 1). The friction between the screw and the upper part to be joined generates heat, which locally plasticizes the material at the joining area. In the following step the element tip penetrates the material and forms, due to its special geometry, a nearly cylindrical extrusion (Step 2). The material is displaced in and against the joining direction, compare Fig. 1. Once the extrusion is fully formed, the speed and axial force are reduced. By using a specific groove zone in the lower section of the fastener, a female metric thread is formed into the previously created hole without any chips (Step 3). At the end of the joining process the fastener is tightened with a defined torque, while the screw head approaches the top of the upper part till contact (Step 4). A force- and form-fitting joint is created.

To achieve high-quality joints, process parameters for the stages have to be set making use of experience and experimental checks (Küting and Hahn, 2004). and (Urbikain et al., 2018) have shown, that the combination of these sequential operations requires adaptation of the process parameters for each step. Once the materials to be joined and the screw are selected, the process window must be determined using the failure torque test. Thereby the fastener is completely screwed in and tightened until reaching the yield strength of the thread. Because of the lower strength compared to the threads of the screw, usually the generated thread of the joined materials fails. Characteristic points are the installation, screw-in and overtorque. Depending on the material and thickness of the parts to be joined, these characteristic torque values may deviate. To ensure high process reliability, the tightening torque should be selected with a clear distance to these torque values. This for example avoids in the case of sheet thickness variations, that the screw is unintentionally tightened with overcritical torque. Additionally, by setting the tightening torque with a distance above the screw-in torque, a premature stop due to an increase of the screw-in torque caused by process fluctuations can be obviated. These considerations result in a practice-relevant process window for the tightening torque, which can vary significantly depending on the material type and thickness of the parts to be joined.

In today's research, e.g. (Costas et al., 2021) combines experimental testing and advanced finite element modeling techniques to study flow-drill screw connections. The mechanical performance of joined aluminum plates with and without pilot holes are analyzed in detail. They show, how extensively the pilot hole increases the ductility and decreases the maximum force of the connection under shear-dominated loading, while the mechanical response under pure tension is only marginally altered.

(Skovron et al., 2015b) investigated the effect of pre-heating the plates with an external source before installing the screws, assessing it with mechanical tests of joints in AA6063-T5A aluminum plates without pilot holes. The authors show that preheating the material reduces the process time and the torque, but they also suggest that the temperature should be limited to prevent harmful effects on the mechanical behavior.

(Küting and Hahn, 2004) and (Skovron et al., 2015a) show that feed force and rotation speed influence each other and have a large impact on the torque values and the geometry of the extrusion. If the feed force is kept constant above the minimum required feed force and the rotation speed is increased, a drop in the torque can be observed, whereby the drop is approximately the same for all the characteristic torque values. The local heat generation at constant rotation speed during the flow drilling step was studied by (Skovron et al., 2015a). The authors substantiate that the generated surface temperature decreases when increasing the force. However, a direct connection between the process parameters and the quality of the formed extrusion is not established.

The experimental studies from (Aslan et al., 2019) and (Küting and Hahn, 2004) reveal that depending on the material and process parameters, different lengths of the extrusion and crack lengths can be observed at the extrusion. If the feed force and the rotation speed are too

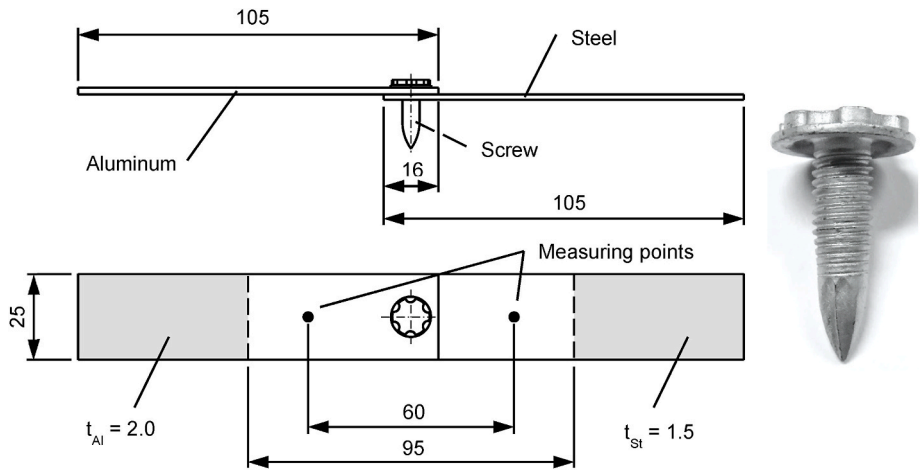

Fig. 2. Geometry of joined specimens and experimental setup for the single-lap shear tests according to DIN EN ISO 14273 (edited from (Graf et al., 2018)). Dimensions given in mm.

Table 1
Technical data of the flow-drill screwing systems.

		Flow-drill screwing system	
Characteristics (max. values)	Unit	Weber RSF 25 (Target system)	Weber RSF 20 S (Initial system)
Torque	Nm	15	15
Rotation speed	rpm	8000	5000
Feed force	kN	3.6	3.6
Downholder force	kN	1.4	1.2

low, no connection can be realized. At sufficient feed force the crack length and the process time decrease approximately linearly with increasing rotation speed. On the other hand, if the feed force is selected too high, a further reduction of the process time can be achieved while increasing the rotation speed, but the crack length remains constant at a high level. Furthermore, if the feed force is too high, there is a risk that the materials deform plastically.

According to (Küting and Hahn, 2004) also the switchover points, see Fig. 1, which corresponds to a certain screw-in depth and at which the adjustable process parameters are changed, are crucial for the joining quality and torque values. High frictional heat is necessary at the beginning of the joining process (Step 1) to enable flow drilling (Step 2). If flow drilling is ended too early, the extrusion and the generated thread are not completely formed or damaged. Exceeding a certain screw-in depth, the induced thermal energy is sufficient. Thereafter, the point switching to screwing (Step 3) should be selected at least after complete forming of the extrusion, as otherwise the process window defined by installation and failure torque becomes too small. In the case of aluminum joining parts, an almost clearance-free thread may be formed with the appropriate process parameters. In the case of steel materials, the degree of thread filling tends to decrease with increasing material strength, even if the choice of parameters is adapted (Küting and Hahn, 2004).

In addition to the process parameters that can be actively influenced, the precise positioning of the components and the clamping forces used also play a decisive role. Other mechanical joining technologies such as punch riveting or clinching, therefore make use of a downholder. On the one hand it holds the materials in position but also positively affects the material flow during the joining process (Meschut et al., 2014). Using the flow-drill screwing technique, there is also the risk of generating a gap between the parts to be joined. To reduce or completely avoid this effect, a downholder is typically installed at the flow-drill screwing systems. The value of the downholder force is essentially dependent on the type and thickness of the clamping and screw-in part, the geometry and coating of the screw. Experimental investigations of (Küting and Hahn, 2004) show that the downholder force is independent from the feed force and rotation speed. In general, higher downholder forces are required with increasing hardness of the materials and thickness of the clamped part.

Once parameters are established for a large number of joints, it is obviously desirable to retain the asset used. Otherwise, it is necessary to transfer and check the parameter sets for target assets. A literature survey revealed no publications concerning the transition to a further developed flow-drill screwing system considering joining process and joint characteristics. As there is a lack of knowledge about the effects on the joint connection in the peer-review literature, thorough experimental studies are required on this topic to achieve a better understanding.

1.2. Methodical approach

As starting point process curves and the joining protocol generated from the initial system are used. Adjustable process steps and parameters of the two different assets are compared in Section 3, in order to transfer the input parameters to the target system. Before implementing the process parameters in the control unit of the target system, a failure torque test is executed, presented in Section 4.1, to review the tightening torque for the specific joining setup. In the next step the necessary parameters for the target system are determined by a parameter optimization, also described in Section 4.1. To qualitatively evaluate the joining results for each process step, after any modification of the parameter sets the produced joints are analyzed by using process curves and cross sections which are correlated with the joining results of the previous optimization loop. The joints are finally validated by single-lap shear tests, see Section 4.2.

2. Experimental set-up

2.1. Materials, fastener and specimen

As upper part an aluminum wrought alloy AlMg4.5Mn0.7, annealed and slightly work-hardened (EN AW-5083 H111), with a thickness of 2.0 ± 0.05 mm was used. A micro-alloyed steel ZStE340 (HC340LA), with a thickness of 1.5 ± 0.05 mm was used as the lower joining partner. Specimens for *single-lap shear* (SLS) testing were produced in accordance with DIN EN ISO 14273. The substrates were joined without using a pre-hole at the center of the overlap, see Fig. 2. The joint was established by the use of a flow-drilling and thread-forming screw (zinc flake coated) made of case-hardened steel according to ISO 7085, manufactured by

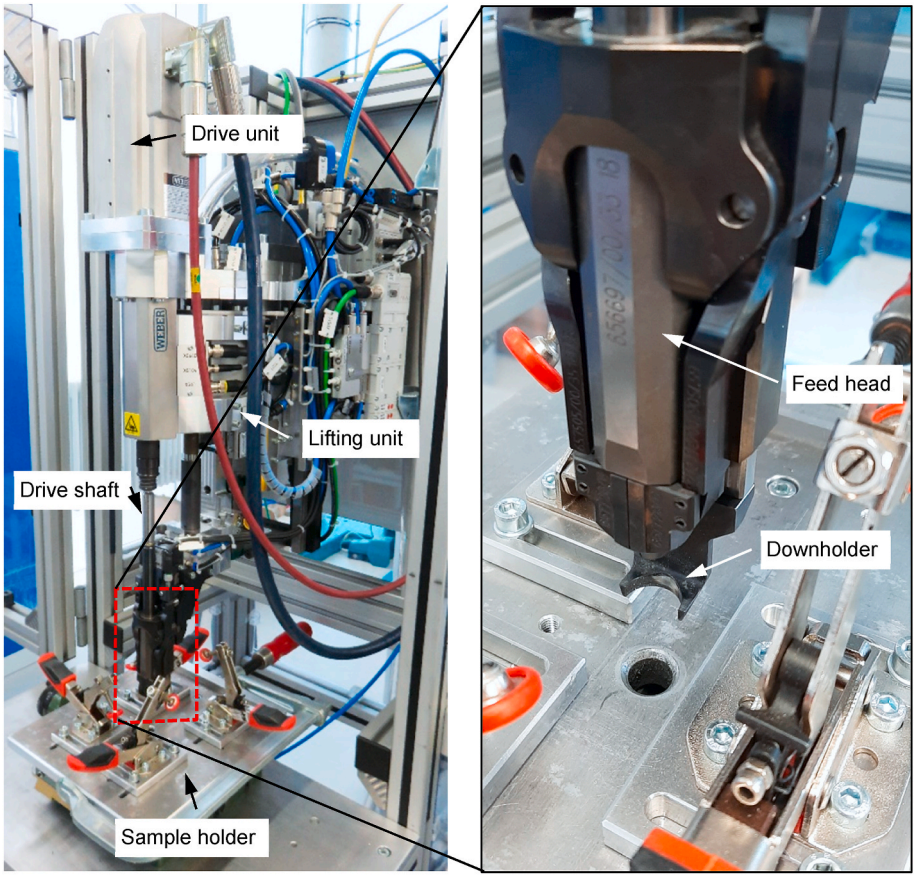

Fig. 3. Flow-dill screwing system Weber RSF 25 (Target system).

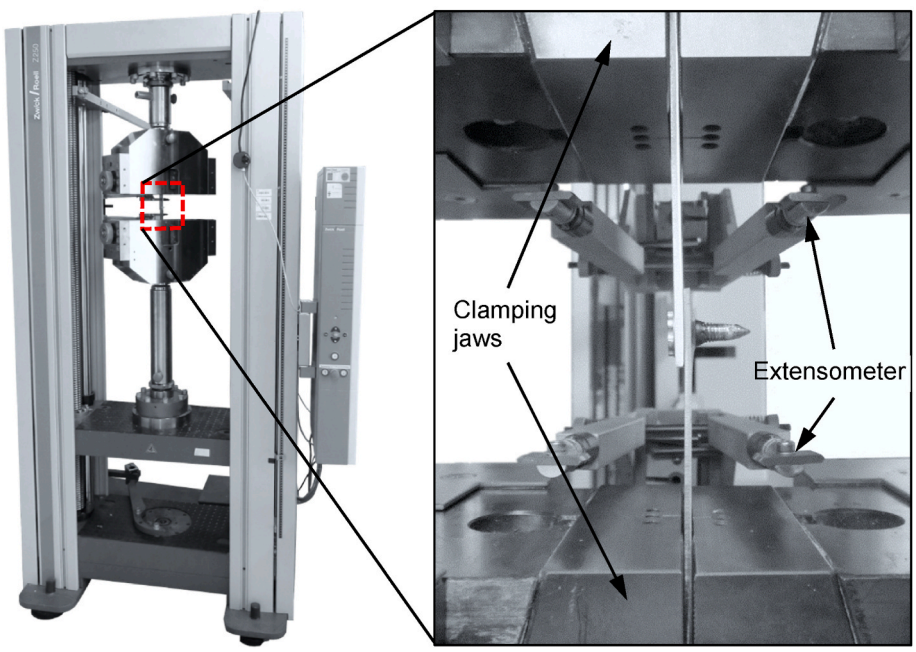

Fig. 4. Universal testing machine Zwick Z250 for mechanical testing according to DIN EN ISO 14273. Clamped SLS-sample and two-arm mechanical extensometer before mechanical testing (edited from (Graf et al., 2018)).

Table 2
Key joining process parameters as inputs for the initial system Weber RSF 20 S with a control unit WSG 100 on the basis of (Graf et al., 2018).

Parameter	Unit	Process step		
		Positioning	Flow-drilling	Screwing & Tightening
Torque	Nm	–	–	12
Rotation speed	rpm	250	3250	1000
Feed force	kN	3.3	3.3	3.3
Depth	mm	16	6	0

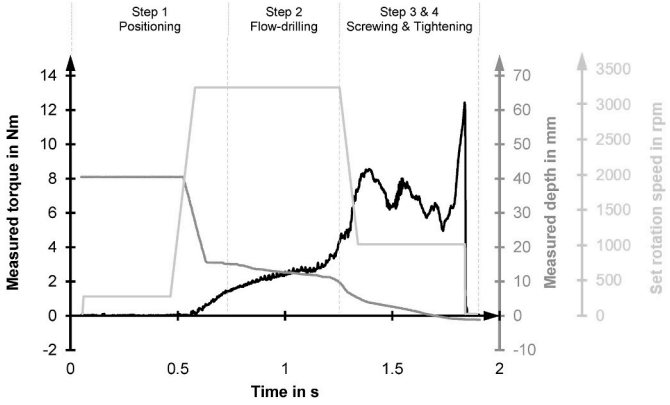

Fig. 5. Representative process curves over time for the initial system (edited from (Graf et al., 2018)).

Table 3
Key joining process parameters as inputs for the target system Weber RSF 25 with a control unit C50RSF V3 after revision on the basis of (Graf et al., 2018).

Parameter	Unit	Process step			
		Positioning	Flow-drilling	Screwing	Tightening
Torque	Nm	–	–	–	12
Rotation speed	rpm	250	3250	1000	1000
Feed force	kN	3.3	3.3	3.3	3.3
Depth	mm	16	6	1.5	0

Table 4
Optimized key joining process parameters as inputs for the target system Weber RSF 25 with a control unit C50RSF V3.

Parameter	Unit	Process step			
		Positioning	Flow-drilling	Screwing	Tightening
Torque	Nm	–	–	–	12
Rotation speed	rpm	250	3250	1000	500
Feed force	kN	–	3.3	3.3	0.6
Depth	mm	16	6	1.5	0

EJOT. It has an M5 thread with a length of 17.0 mm and a Torx Plus 12 EP (External Plus) head with an outer diameter of 11.8 mm.

2.2. Flow-drill screwing systems

The samples were joined with two different flow-drill screwing systems. Technical characteristics are shown in Table 1. Both are commonly used in the automotive industry. As initial system, a flow-drill screwing system Weber RSF 20 S with a control unit WSG 100 was used.

As target system, a flow-drill screwing system Weber RSF 25 with a control unit C50RSF V3 was used, see Fig. 3. The respective control unit was used for the adjustment of the process parameters and generation of the process curves (torque, depth, rotational speed).

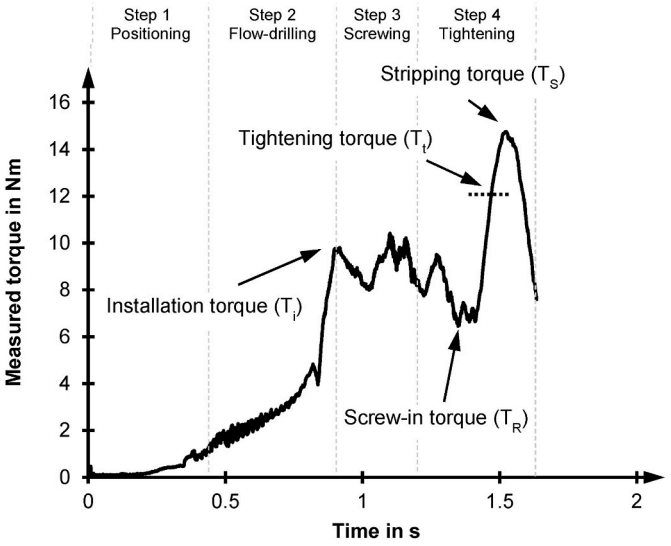

Fig. 6. Representative process curve of the failure torque test at the target system for determination of the tightening torque.

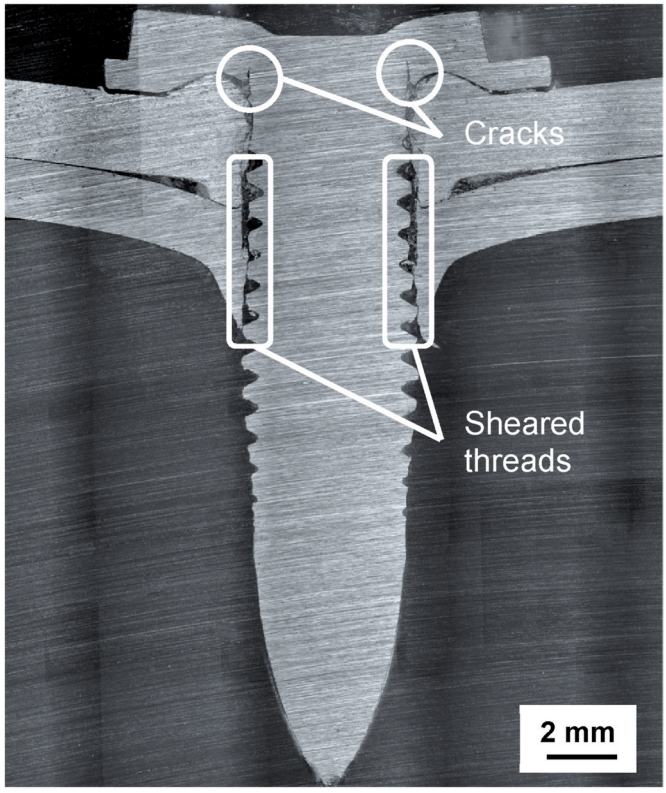

Fig. 7. Cross section of the joint after failure torque test with the target system.

2.3. Microscopic imaging and mechanical testing

In order to determine the process parameters and characterize the quality of the hybrid joints, cross sections through the center of the screw were prepared by using an epoxy based mounting resin VersoCit-2 from Struers GmbH. For evaluation a light optical microscope Olympus GX51, equipped with a digital camera of type ColorView 3.2 MP CCD in bright field illumination was used. Representative images, taken with the above mentioned light optical microscope, were quantitatively analyzed using the Olympus Stream Essentials Version 1.9 evaluation

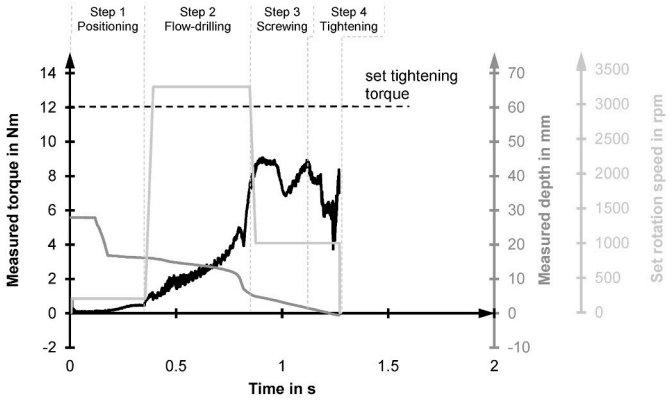

Fig. 8. Representative process curves over time generated with the target system. Key joining process parameters from Table 3.

software.

Mechanical testing was conducted according to DIN EN ISO 14273 (dimensions see Fig. 2) with a traverse speed of 5 mm/min on a universal testing machine Zwick Z250 till 80% drop in load. Avoiding slipping during testing, the samples were fixed at the grey-shaded areas in Fig. 2 using mechanical clamping jaws. During the loading of the joint, the force and the local relative displacement were measured. In Fig. 2 the measuring locations for local displacements are indicated by black points for the initial position of the two-arm mechanical extensometer, which is also displayed in Fig. 4.

3. Revision of process parameters for target system (from previous publication using initial system)

The aim of the following investigations was to identify the input parameters for each joining step from the initial flow-drill screwing system. In a previous work, Graf et al. (2018), already assumed the

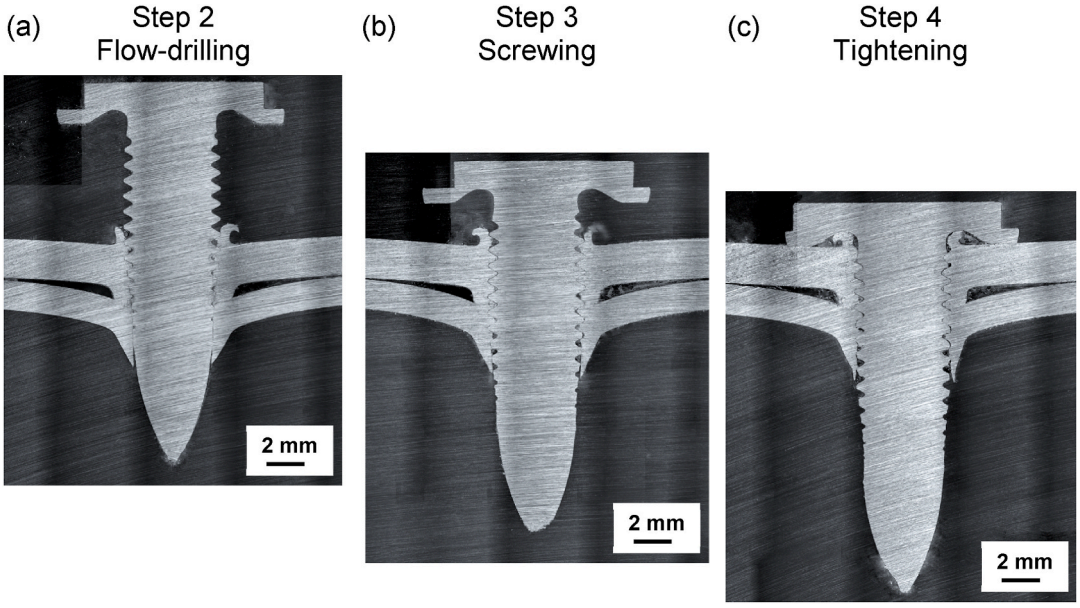

Fig. 9. Cross sections of the joint at the end of the process steps generated with the target system by using the parameter set from Table 3. Flow-drilling (a), screwing (b) and tightening (c).

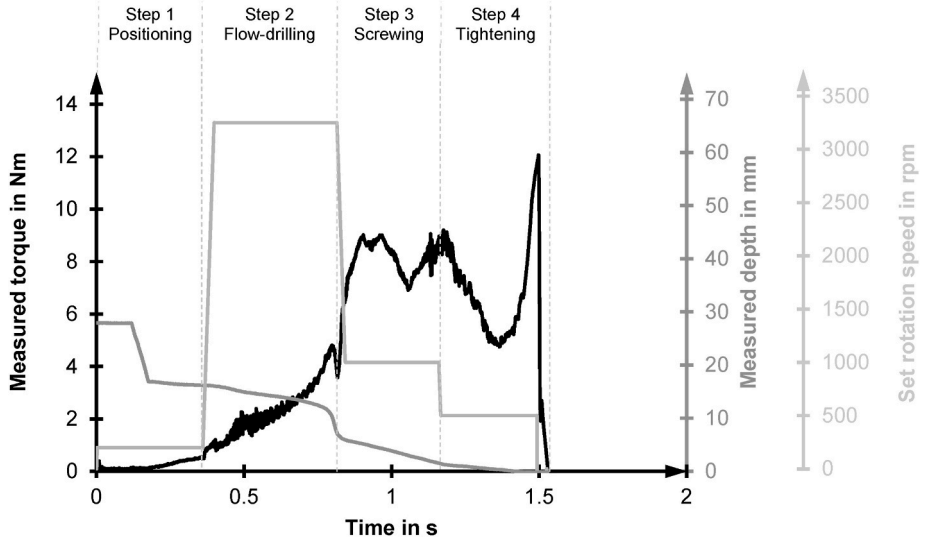

Fig. 10. Representative process curves over time generated with the target system. Optimized key joining process parameters from Table 4.

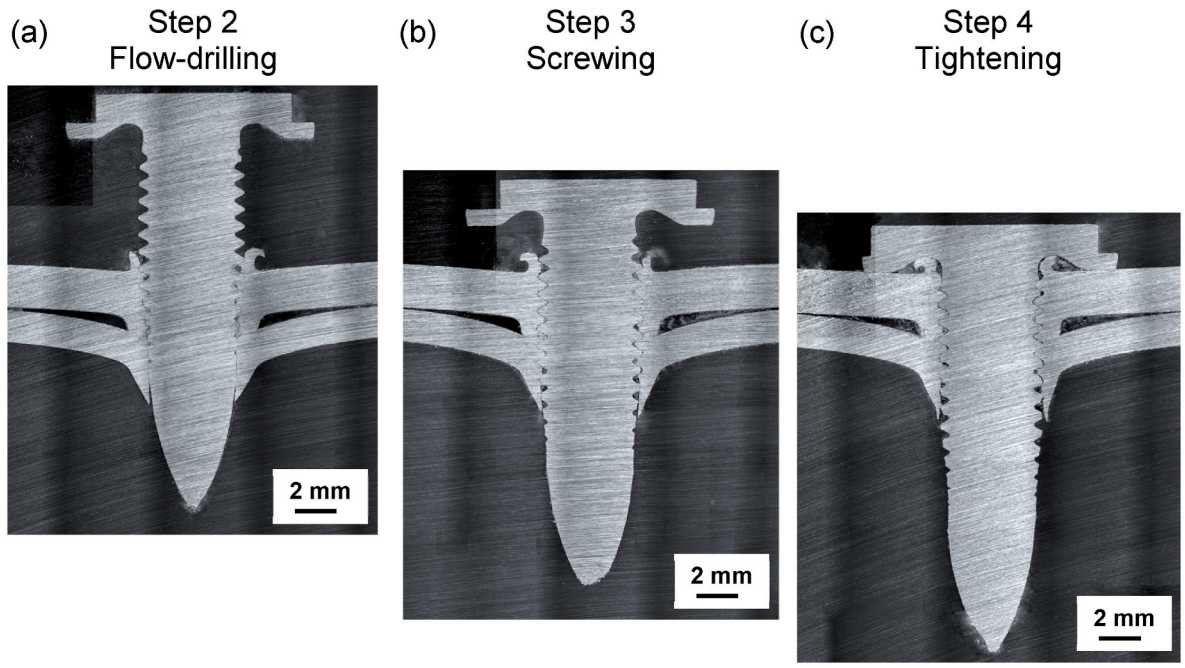

Fig. 11. Cross sections of the joint at the end of the process steps generated with the target system by using the optimized parameter set from Table 4. Flow-drilling (a), screwing (b) and tightening (c).

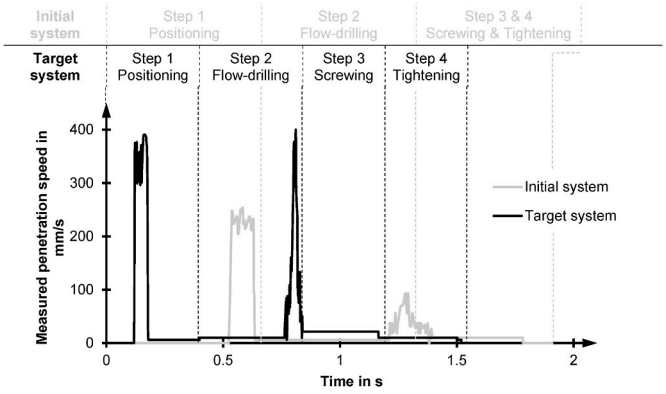

Fig. 12. Penetration speed over time generated with the initial system and target system by using the optimized parameter set from Table 4.

required process parameters (see Table 2) for sufficiently joining the materials mentioned above using the initial system. On this basis the optimized joining parameters for the target system were determined (see Table 4). First of all, the process curves and the joining protocol optimized for and generated by the initial joining system were used at the target system. Fig. 5 shows the representative process curves over time of one successful joining process (Graf et al., 2018). Experimental investigations have shown that the target values for the rotation speed are met on both systems. Due to this fact and for purpose of comparison the rotation speed is displayed as set value hereafter. Torque and depth are shown as measured values. The different joining steps are indicated at the top of the diagram. Comparing input parameters of the two different assets considered, the adjustable process steps and parameters differ. In the specific control unit, the joining process of the initial flow-drill screwing system consists of three adjustable joining steps: Positioning (Step 1), flow-drilling (Step 2) and screwing/tightening (Step 3), see Table 2. Compressing the presented steps during the flow-drill screwing process, shown in Fig. 1, screwing and tightening are combined into one step. In contrast, in the control unit of the target flow-drill screwing system, these two steps are independently adjustable, to enable precise tightening.

As a starting point, for both steps (screwing and tightening) the same process parameters were assumed, see Table 3. This parameter set served as basis to experimentally determine the final process parameters for the control unit of the target system.

4. Experimental results with target system

4.1. Determination of process parameters for target system

Before implementing the process parameters in the control unit of the target flow-drill screwing system, a failure torque test was conducted at the target system to review the tightening torque for the specific joining setup. In this test, the screw is loaded until failure, i.e. until torque drops (Küting and Hahn, 2004). Fig. 6 shows a representative process curve of the torque with characteristic points of the respective joining steps. In step one, the torque increases while the material warms up. At the end of process step two (flow-drilling), the torque reaches the installation torque (T_i)[1] at 9.8 Nm. In the following step (screwing) the torque decreases till reaching the screw-in torque (T_R)[1] at 6.5 Nm during the last process step (tightening). Finally, the torque strongly increases up to point of stripping torque (T_S)[1] at 15 Nm. For the example steel-aluminum joint, this maximum torque is indicated by shearing of the threads, strong plastic deformation and cracking of the screw head, see Fig. 7. The calculated tightening torque (T_t),[1] see Fig. 6, for the specific joining setup can be set to 12 Nm,[2] which confirms the assumptions for the initial system, compare Table 2.

As obvious next step, the parameter set chosen in Table 3 is applied to create the example joint. In Fig. 8, representative process curves over time generated with the target system are shown. Additionally, the target tightening torque for the last process step „Tightening" is indicated by a dashed line. Having a closer look at the process curve of the

[1] Index according to (DVS/EFB-Gemeinschaftsausschuss "Mechanisches Fügen" (2021)).

[2] The tightening torque is chosen in the range described by $1.2 \times T_i \leq T_t \leq 0.85 \times T_s$ (DVS/EFB-Gemeinschaftsausschuss "Mechanisches Fügen" (2021)).

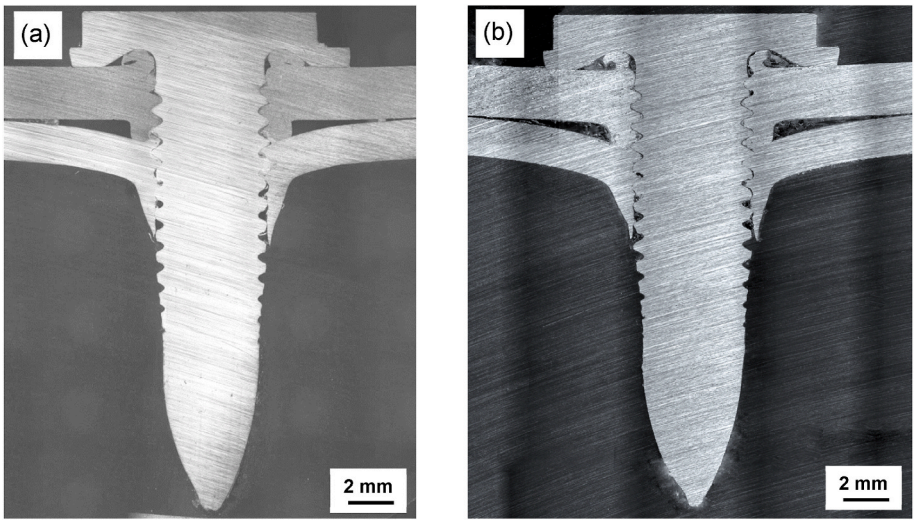

Fig. 13. Cross section of the joint generated with the initial system (Graf et al., 2018) (a) and with the target system by using the optimized parameter set from Table 4 (b).

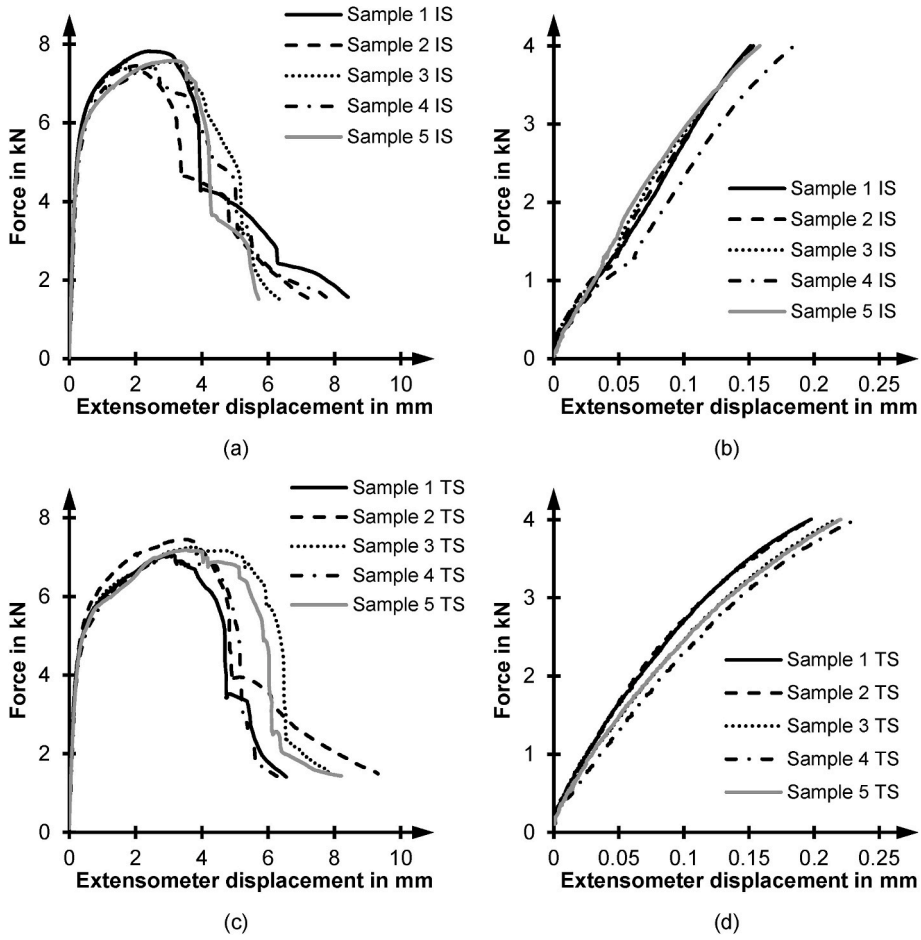

Fig. 14. Force-displacement curves of aluminum-steel flow-drill connections joined with the initial (Graf et al., 2018) (a) and target system (c). Detailed view of the corresponding starting phase initial (b) and target system (d). Single-lap shear test according to DIN EN ISO 14273.

torque, it can be seen, that the set tightening torque of 12 Nm is not reached. Fig. 9 (a) - (c) displays representative cross sections of the joint at different process steps generated with the target system. In Fig. 9 (a) it can be seen, that the extrusion is fully formed without any damages at the element dip after completing the process step flow-drilling. A complete female thread is generated during screwing. The thread flanks of the screw are nearly completely covered by the joined materials and are in good shape, as seen in Fig. 9 (b). Having a closer look at the cross-section, shown in Fig. 9 (c), also after tightening an almost clearance-free thread is achieved. However, it can be observed, that the

Table 5
Mechanical test results achieved with the initial (Graf et al., 2018) and target system.

Parameter	Unit	Initial system	Target system
Average strength value	N	7574.7	7198.3
Maximum value	N	7818.1	7452.7
Minimum value	N	7453.6	7042.2
Plus	N	243.4	254.3
Minus	N	121.1	156.1
Variance	N^2	17523	23640
Standard deviation	N	132.4	153.8
Average energy absorption	J	36.5	39.5

displayed in Fig. 13 (b) in comparison to the one achieved with the initial system Fig. 13 (a). Joining with the experimentally determined process parameters enables defined tightening and leads to an optically good joining connection, see Fig. 13 (b). The head of the flow-drill screw is in contact with the surface of the clamped part, while receiving the material of the clamped part displaced to the top. Furthermore, the threads of the screw are homogenously filled, even at the extrusion, without any visual damages. Having a closer look at the extrusion, the degree of thread filling decreases at the screw-in part. Moreover, it can be observed, that the position of the clamped part slightly deviates from horizontal orientation. The clamped part (and with that also the screw-in part) is bent towards the tip of the screw.

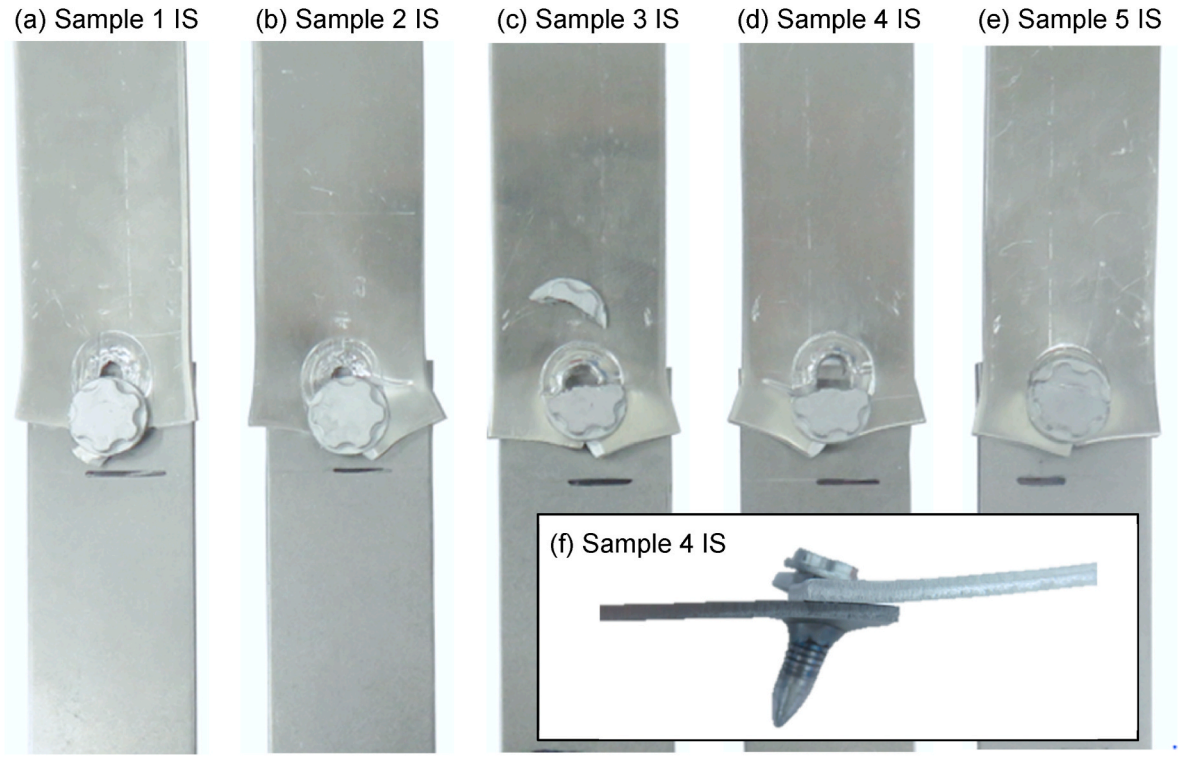

Fig. 15. Fracture pattern after mechanical testing according to DIN EN ISO 14273. Samples generated with the initial system. (a)–(e) Combination of tear out failure clamped part and failure of the screw. (f) Side view Sample 4 IS (Graf et al., 2018).

positioning of the clamped part deviates from horizontal orientation. The clamped part (and with that also the screw-in part) is bent towards the tip of the screw, while exceeding the target value for the depth.

On this basis, an iterative loop was carried out to optimize the joining process parameters of the last step tightening. In order to guarantee a defined tightening at the end of the joining process, the feed force was significantly reduced to 0.6 kN and the rotation speed to 500 rpm (see Table 4). The resulting process curves over time generated with the optimized parameter set at the target flow-drill screwing system are shown in Fig. 10. The tightening torque and depth are observed precisely, while generating the joint connection in 1.5 s. Fig. 11 (a) – (c) displays representative cross sections of the joint after the different process steps flow-drilling, screwing and tightening generated with the target system. The used optimized process parameters can be extracted from Table 4.

Penetration speed over time at the different joining steps is exemplarily shown in Fig. 12 for both flow-drill screwing systems. It can be observed, that during positioning up to two times and during flow-drilling up to four times higher speeds are driven at the target system. During the other process steps screwing and tightening the penetration speeds are similar.

The final result of the joint, produced at the target joining system, is

4.2. Mechanical validation of the joints obtained with the target system

Five SLS-samples, generated with the optimized joining process parameters for the target system, were tested. Fig. 14 and Table 5 contain the mechanical test results comparing joints produced at the initial (a) - (b) and the target system (c) - (d), presented as force-displacement curves. The maximum load and the displacement at failure load are very similar. An average strength value of 7198.3 $N\,^{+254.3}_{-156.1}$ was achieved.[3] Compared to the results achieved with the initial system, a higher average energy absorption at higher variance was obtained. Having a closer look on the slope at the beginning of the force-displacement curves (b) and (d), the increase in force occurs with larger covered path for samples joined with the target system. The fracture analysis after mechanical testing, see Fig. 16, shows, that the specimens fail via bending up of the plate edge with failure of the screw in combination with a tear out of the aluminum sheet. The same fracture pattern was identified for samples joined with the initial system, see

[3] With the initial flow-drill screwing system an average strength value of 7574.7 $N\,^{+243.4}_{-121.1}$ was achieved.

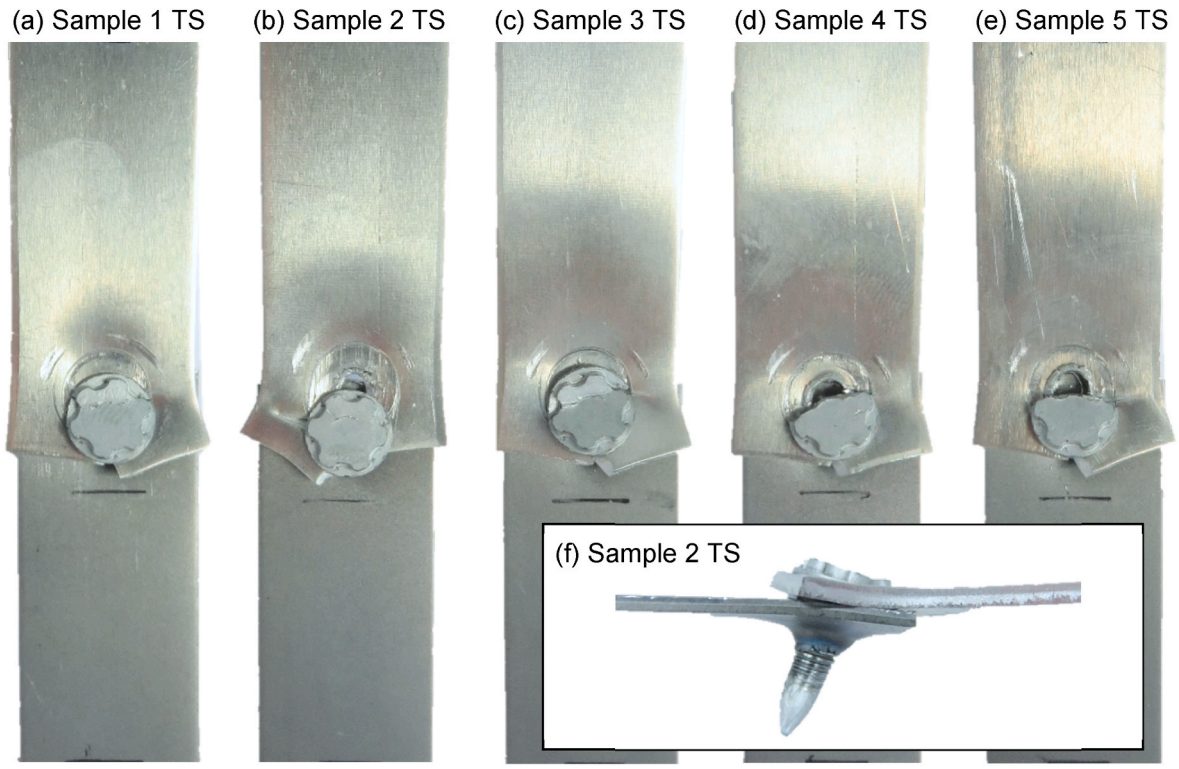

Fig. 16. Fracture pattern after mechanical testing according to DIN EN ISO 14273. Samples generated with the target system. (a)–(e) Combination of tear out failure clamped part and failure of the screw. (f) Side view Sample 2 TS.

Fig. 15.

5. Discussion

To experimentally determine the final process parameters for the target system, the joining protocol and process curves generated with the initial system offer a good starting point (Section 3). The necessary testing effort can be reduced since for the process steps positioning, flow-drilling and screwing (Step 1–3) no significant adjustments are required for implementation, compare Section 4.

5.1. Revision of process parameters for target system

Implementing the process parameters of the initial system in the target system has shown, that due to differences in the process guidance a revision of the process parameters is necessary (Section 3).

In contrast to the initial system, in the control unit of the target system the process step tightening (Step 4) is implemented as separate adjustable stage, see Table 3. Due to this an assumption must be made on the basis of the process curves, see Fig. 5, generated with the initial system.

In this work, except for the feed force, all necessary values are adapted from the already known process curves. Consequently, initially the feed force was set equal to the previous process step, screwing (Step 3), see Table 3, in order to start off with the parameter settings of the initial system. Section 4.1 shows that this trivial assumption has to be modified.

5.2. Determination of process parameters for target system

The failure torque tests performed at the target system verify the tightening torque for the specific joining setup. However, the process curves generated with the process parameters after revision (see Table 3) have shown, that the set tightening torque is not reached (see Fig. 8). The reason for remaining below the target value is the high feed force (3.3 kN) combined with the high rotation speed (1000 rpm) in the last process step tightening. The effect is that defined tightening, in accordance with the threshold value for the depth, is not possible. Due to exceeding the threshold value for the depth, the clamped and screw-in part are bent towards the tip of the screw. In addition, using high feed forces for tightening leads to shearing of the thread flanks (Meschut, 2013). This means that the torque cannot be transmitted at this point.

Reducing the feed force and rotation speed (see Table 4) guarantees a precise tightening at the end of the joining process, as shown in Fig. 10. Furthermore, compared to the joining process of the initial system, the time needed for sufficient joining, is significantly shortened (initial system: 1.86 s; target system: 1.53 s). Mainly caused by faster positioning (step 1) and the shorter flow-drilling phase (step 2), due to quicker switchover and reaching of the rotation speed between the process steps. Consequently, also the heat input generated in the joining zone is reduced. Cross sections of the joint connection are showing a high degree of thread filling, even at the screw-in part made of micro-alloyed steel. To sum it up, a qualitatively good joint is produced, see Fig. 13 (b). The reduced degree of thread filling, even if the choice of parameters is adapted, is typically in the case of steel materials and was also noticed by Küting et al. (Küting and Hahn, 2004).

5.3. Mechanical validation and fracture patterns

The fracture analysis of the produced specimens, shown in Fig. 16, reveals the same failure mode as the specimens generated with the initial system (see Fig. 15), while achieving nearly the same shear-strength at higher energy absorption. It is reasonable to assume, that due to the fact that the position of the clamped part slightly deviates from horizontal orientation, see Fig. 12 b), the head of the screw already fails at lower loads. Compared to the results obtained with the initial system, this leads to smaller shear-strengths of the joints generated with the target system. In comparison to the flow-drill connection

investigated by Sønstabø et al. (Sønstabø et al., 2015), a different failure mode was observed for the single-lap shear test. In Sønstabø et al., rotation of the screw due to the shear force led to a one-sided thread engagement and a through-thickness shear fracture of the bottom sheet material (Upper and lower joining materials: EN AW-6016 T4 with a thickness of 2.0 mm. Fastener: M4 screw with a length of 10.0 mm, made of case-hardened mild steel, manufactured by EJOT). In contrast to the experiments carried out in this work, the screw remains in the clamped part. The different failure mode is caused by the lower strength of the aluminum sheet compared to the steel sheet, used as screw-in part.

Having a closer look at the force-displacement curves (see Fig. 14), samples joined with the experimentally determined process parameters on the target system fail at higher extensometer displacement, compared to samples joined with the initial joining system and corresponding parameter set. Consequently, it is reasonable to assume, that due to the lower heat input at the joining zone, caused by the shorter flow-drill step as well as the reduction of the feed force and rotation speed, a more compliant behavior of the joint is achieved. This leads to a higher energy absorption of the joint.

6. Conclusion

In this study, a methodical procedure for the transition to a further developed flow-drill screwing system is shown exemplarily. Based on an initial flow-drill screwing system and process parameter set an experimental program was carried out to identify necessary modifications in the process guidance step by step.

In order to determine the necessary process parameters for the target system, in a first step the parameter settings of the initial system were implemented in the target system. For the example in this study, the process curves and the joining protocol generated from the initial joining system were used. To review the tightening torque for the specific joining setup, a failure torque test was conducted at the target system. Then, the documented straight-forward methodological approach was carried out to optimize the parameter set. To qualitatively evaluate the joining results for each step, after any modification of the parameter sets the produced joints were analyzed by using process curves (torque, depth, rotational speed) and cross sections which were correlated with the results of the step before. Finally, the created joints were validated by using mechanical tests. The following conclusion can be drawn:

- It was shown, that using the process parameters generated with the initial system offers a good starting position and significantly reduces the experimental effort needed to determine the optimal process parameters for the target flow-drill screwing system. However, a simple transfer of the parameter set without any adjustments and additional test series for validation is not possible.
- Due to the separate process step tightening and the process parameters that are additionally available at the target system, a better process control in the last joining step tightening is possible. A precise tightening, as specified in the joining program, is guaranteed.
- The transition to the further developed flow-drill screwing system enables faster joining, while achieving approximately the same tensile shear strength at nearly the same variance, as with the initial system. Additionally, a more compliant behavior of the joint is established, resulting from reduced heat impact in the joining zone generated during the process.

Acknowledgments

This study was performed within the research project NGC (Next Generation Car) at the DLR-Institute of Vehicle Concepts.

References

Aslan, F., Langlois, L., Balan, T., 2019. Experimental analysis of the flow drill screw driving process. Int. J. Adv. Manuf. Technol. 104, 2377–2388. https://doi.org/10.1007/s00170-019-04097-z.

Costas, M., Morin, D., Sønstabø, J.K., Langseth, M., 2021. On the effect of pilot holes on the mechanical behaviour of flow-drill screw joints. Experimental tests and mesoscale numerical simulations. J. Mater. Process. Technol. 294, 117133 https://doi.org/10.1016/j.jmatprotec.2021.117133.

DVS/EFB-Gemeinschaftsausschuss, Fügen, Mechanisches, 2021. Merkblatt DVS/EFB 3445-1 Fließlochformendes Schrauben.

Friedrich, H.E., 2013. Leichtbau in der Fahrzeugtechnik. Springer Fachmedien Wiesbaden, Wiesbaden.

Graf, M., Sikora, S.P., Roider, C.S., 2018. Macroscopic modeling of thin-walled aluminum-steel connections by flow drill screws. Thin-Walled Struct. 130, 286–296. https://doi.org/10.1016/j.tws.2018.02.023.

Groche, P., Wohletz, S., Brenneis, M., Pabst, C., Resch, F., 2014. Joining by forming—a review on joint mechanisms, applications and future trends. J. Mater. Process. Technol. 214, 1972–1994. https://doi.org/10.1016/j.jmatprotec.2013.12.022.

Hahn, O., Freymüller, C., 2017. Weiterentwicklung der Eigenschaften von fließloch- und gewindefurchenden Schrauben zur Erweiterung der Einsatzgrenzen für die Stahl-Aluminium-Mischbauweise. Shaker Verlag, Aachen.

Küting, J., Hahn, O., 2004. Entwicklung des Fließformschraubens ohne Vorlochen für Leichtbauwerkstoffe im Fahrzeugbau. Shaker Verlag, Aachen.

Martinsen, K., Hu, S.J., Carlson, B.E., 2015. Joining of dissimilar materials. CIRP Annals 64, 679–699. https://doi.org/10.1016/j.cirp.2015.05.006.

Meschut, G., 2013. Eignung von Loch und Gewinde formenden Schrauben zum Fügen von Mehrblechverbindungen. Ergebnisse eines Vorhabens der industriellen Gemeinschaftsforschung, EFB, Hannover.

Meschut, G., Janzen, V., Olfermann, T., 2014. Innovative and highly productive joining technologies for multi-material lightweight car body structures. J. Mater. Eng. Perform. 23, 1515–1523. https://doi.org/10.1007/s11665-014-0962-3.

Schindler, V., Sievers, I., 2008. Forschung für das Auto von Morgen. Aus Tradition entsteht Zukunft. Springer-Verlag, Berlin, Heidelberg.

Skovron, J., Mears, L., Ulutan, D., Detwiler, D., Paolini, D., Baeumler, B., Claus, L., 2015a. Characterization of flow drill screwdriving process parameters on joint quality. SAE Int. J. Mater. Manf. 8, 35–44. https://doi.org/10.4271/2014-01-2241.

Skovron, J.D., Rohan Prasad, R., Ulutan, D., Mears, L., Detwiler, D., Paolini, D., Baeumler, B., Claus, L., 2015b. Effect of thermal assistance on the joint quality of Al6063-T5A during flow drill screwdriving. J. Manuf. Sci. Eng. 137 https://doi.org/10.1115/1.4031242.

Sønstabø, J.K., Holmstrøm, P.H., Morin, D., Langseth, M., 2015. Macroscopic strength and failure properties of flow-drill screw connections. J. Mater. Process. Technol. 222, 1–12. https://doi.org/10.1016/j.jmatprotec.2015.02.031.

Urbikain, G., Perez, J.M., López de Lacalle, L.N., Andueza, A., 2018. Combination of friction drilling and form tapping processes on dissimilar materials for making nutless joints. Proc. IME B J. Eng. Manufact. 232, 1007–1020. https://doi.org/10.1177/0954405416661002.